https://doi.org/10.21122/2227-1031-2024-23-2-151-162

UDC 629.331.03-83-592.3

The Influence of Road Adhesion Coefficient on Energy Consumption and Dynamics of Battery Electric Vehicles

Le Thanh Nhan[1)], Dam Hoang Phuc[1)], Le Hue Tai Minh[1, 2)], S. V. Kharytonchyk[3)], V. A. Kusyak[3)], Nguyen Thanh Cong[4)]

[1)]Hanoi University of Science and Technology (Hanoi, Socialist Republic of Vietnam),
[2)]University of Science and Technology of Hanoi (Hanoi, Socialist Republic of Vietnam),
[3)]Belarusian National Technical University (Minsk, Republic of Belarus),
[4)]University of Transport and Communications (Hanoi, Socialist Republic of Vietnam)

Abstract. Currently, in economically developed countries, electric vehicles are considered as a solution to the problematic issue of reducing greenhouse gas emissions from road vehicles. The level of energy consumption is a critical factor in determining the overall performance of an electric vehicle. The article analyzes the influence of tire adhesion coefficient on the energy consumption of a battery electric vehicle when operating in typical standard driving cycles. In order to estimate the energy consumption during driving with different tire adhesion coefficients an electric vehicle longitudinal dynamic model is used, which allows taking into account various driving modes (Eco, Comfort, Sport) and sliding of the drive wheels in contact with the road surface. The proposed model, based on submodels of such main components of an electric vehicle as an electric motor and a traction battery, includes tire and vehicle body dynamics submodels, as well as a human-driver submodel with PID controller in the control circuit to track given trajectories. A series of experiments with the VinFast Vf e34 passenger electric vehicle on a dynamometer test bench were carried out to determine the electric motor's performance characteristics at various operating modes and identify many other input parameters for simulation and verifying the mathematical model accuracy. The simulation results of the distance traveled by an electric vehicle on a single charge are compared with the manufacturer's experimental data during operating the test vehicle in the standard European driving cycle. Simulation scenarios with different accelerating modes are proposed to analyze the influence of the adhesion coefficient on the EV's dynamic characteristics and the level of energy consumption. The simulation results on the determination of the energy consumed by an electric vehicle when moving in various driving cycles with road adhesion coefficients are presented in the activity. The given results show the significant impact of the adhesion coefficient on electric vehicle energy consumption in various standard driving cycles, especially on low-grip roads.

Keywords: battery electric vehicle, traction electric motor, energy consumption, tire adhesion coefficient, vehicle dynamics, standard European driving cycles, computer modeling

For citation: Le Thanh Nhan, Dam Hoang Phuc, Le Hue Tai Minh, Kharytonchyk S. V., Kusyak V. A., Nguyen Thanh Cong. (2024) The Influence of Road Adhesion Coefficient on Energy Consumption and Dynamics of Battery Electric Vehicles. *Science and Technique*. 23 (2), 151–162. https://doi.org/10.21122/2227-1031-2024-23-2-151-162

Адрес для переписки
Дам Хоанг Пхук
Ханойский университет науки и технологий
ул. Дай Ко Вьет, 1,
100000, г. Ханой, Вьетнам
Тел.: +84 932367577
Phuc.damhoang@hust.edu.vn

Address for correspondence
Dam Hoang Phuc
Hanoi University of Science and Technology
1, Dai Co Viet Street,
100000, Ha Noi, Viet Nam
Tel.: +84 932367577
Phuc.damhoang@hust.edu.vn

Влияние коэффициента сцепления шин с дорогой на потребляемую энергию и динамику аккумуляторных электромобилей

Асп. Ле Тхань Нань[1)], канд. техн. наук, доц. Дам Хоанг Пхук[1)], асп. Ле Хуэ Тай Минь[1, 2)], докт. техн. наук, проф. С. В. Харитончик[3)], кандидаты техн. наук, доценты В. А. Кусяк[3)], Нгуен Тхань Конг[4)]

[1)]Ханойский университет науки и технологий (Ханой, Социалистическая Республика Вьетнам),
[2)]Университет науки и технологий Ханоя (Ханой, Социалистическая Республика Вьетнам),
[3)]Белорусский национальный технический университет (Минск, Республика Беларусь),
[4)]Университет транспорта и коммуникаций (Ханой, Социалистическая Республика Вьетнам)

Реферат. В настоящее время в экономически развитых странах электромобили рассматриваются как решение проблемного вопроса по сокращению выбросов парниковых газов от мобильных транспортных средств. Уровень потребляемой энергии электромобилем является решающим фактором, определяющим общую производительность транспортного средства на электрической тяге. В статье анализируется влияние коэффициента сцепления шин с дорогой на потребляемую энергию аккумуляторным электромобилем при эксплуатации в типичных стандартных ездовых циклах. Для оценки потребляемой энергии при движении с различными коэффициентами сцепления шин используется продольная динамическая модель электромобиля, позволяющая учитывать различные режимы вождения («эко», «комфорт», «спорт») и скольжение ведущих колес в контакте с дорожным покрытием. Разработанная модель, построенная на основе субмоделей таких основных компонентов электромобиля, как электрический двигатель и тяговая аккумуляторная батарея, включает субмодели динамики шин и кузова, а также субмодель логики действий водителя с ПИД-регулятором в цепи управления для отслеживания заданных траекторий движения транспортного средства. Для определения внешних рабочих характеристик тягового электродвигателя на различных режимах работы силового агрегата и идентификации ряда других входных параметров для математического моделирования и оценки адекватности имитационной модели была проведена серия экспериментов с легковым электромобилем VinFast Vf e34 на динамометрическом испытательном стенде. Результаты моделирования по максимальному пройденному расстоянию электромобилем на одном заряде батарей сопоставляются с экспериментальными данными завода-производителя при эксплуатации испытуемого автомобиля в стандартном европейском ездовом цикле. Предлагаются сценарии моделирования процессов разгона с различными режимами ускорения для анализа влияния коэффициента сцепления шин с дорогой на динамические характеристики электромобиля и уровень потребляемой энергии. Приводятся результаты компьютерных экспериментов по определению потребляемой электромобилем энергии при движении в различных ездовых циклах с различными коэффициентами сцепления шин с опорной поверхностью дорожного покрытия. Полученные результаты показывают значительное влияние коэффициента сцепления шин на расход потребляемой электромобилем энергии в различных ездовых циклах, особенно на дороге с низким коэффициентом сцепления.

Ключевые слова: аккумуляторный электромобиль, тяговый электродвигатель, потребляемая энергия, коэффициент сцепления шин с дорогой, динамика автомобиля, стандартные европейские ездовые циклы, компьютерное моделирование

Для цитирования: Влияние коэффициента сцепления шин с дорогой на потребляемую энергию и динамику аккумуляторных электромобилей / Ле Тхань Нань [и др.] // *Наука и техника.* 2024. Т. 23, № 2. С. 151–162. https://doi.org/10.21122/2227-1031-2024-23-2-151-162

Introduction

Given the current air pollution, electric vehicles (EVs) are currently considered as one of the solutions to reduce greenhouse gas emissions. Recently, many large companies have focused on developing environmentally friendly cars and have also achieved many successes with a large number EVs sold [1, 2]. However, the major problem with electric cars is that the distance traveled on a single charge does not meet consumers' needs. Many studies have been conducted on the EV's energy consumption (EC), such as the optimization of energy management, vehicle's available energy usage [3–6], regenerative braking [7–9], and other operating parameters on EC [8, 10–12].

Research [3] shows that the combined use of two energy sources, namely supercapacitors and batteries, can extend battery life. The LQG control algorithm makes it possible to reduce the average current during vehicle operation by 18,9 % (from 34,3 A to 27,8 A), thus reducing energy consumption. However, this study did not consider the external condition's that influence on the Ev's energy consumption.

In research [7], strategies for controlling the regenerative braking system during vehicle movement are proposed with different objectives. The research results show that the vehicle braking process from a velocity of 100 km/h to a complete stop with an optimal regenerative energy control strategy can increase the amount of regenerative energy by 84,4 % compared to the standard control strategy. In addition, the braking distance was 13,2 % shorter. This study also did not investigate the effectiveness of regenerative braking control strategies under low adhesion coefficient conditions.

The research [10] shows the influence of the driver on the energy consumption of the vehicle through real-time data collection and analysis. The article provides parameters to be evaluated by driving, which evaluates and analyzes the impact of these parameters on energy consumption. Nevertheless, the research was conducted only on roads with good adhesion coefficients. The research [11] also shows the significant dependence of the electric motor (EM) power demand and EC on the driving styles. However, these studies have only focused on energy issues in EVs themselves without considering the influence of external parameters on EC, especially the tire adhesion coefficient.

In terms of internal combustion engine (ICE) vehicles, studies on the adhesion coefficient mainly focus on its influence on dynamics control to enhance vehicle safety and efficiency [13–15], not on the vehicle's fuel or energy consumption in certain driving cycles.

Therefore, this article analyzes the influence of the tire adhesion coefficient on EV's energy consumption and dynamic characteristics when operating in different driving cycles. The research methodology consists of vehicle simulation in combination with real experiments to determine the input information and verify the accuracy of the model, thereby enabling surveys and analysis of the EV performance in various operating conditions. An EV longitudinal dynamic model with all of the EV powertrain components is built to study the vehicle dynamics performance and energy consumption in different road adhesion conditions. Real experiments on the dynamometer are performed to collect the input parameters for the simulation and verify the mathematical model's accuracy. Finally, the results of the vehicle dynamic characteristics and energy consumption after simulating by the proposed model on various roads with different tire adhesion coefficients are analyzed.

Research method

V*ehicle simulation model.* To achieve the purpose of the research the electric vehicle simulation model (Fig. 1) was developed, which includes the submodels of driving cycle, electric motor, traction battery, braking system, active/passive tires dynamics, and vehicle body dynamics [16]. The simulation of the EV operating process by given driving cycles can be done on the proposed model.

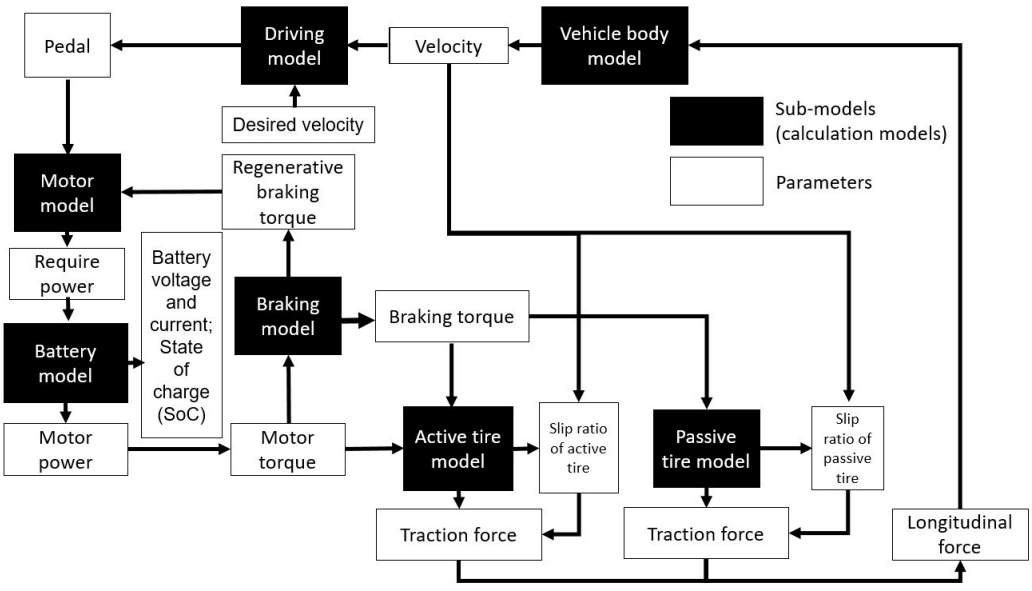

Fig. 1. Electric vehicle models

The above EV submodels were based on [7, 17], including the tire models to calculate the tire slip ratio, the battery model based on SOC percentage, the load-efficiency curve, and the relationship between the pedal signal and driving mode. Each submodel is described as follows.

The vehicle body dynamic submodel, based on the classic equations of ground vehicles theory, is shown in Fig. 2. The longitudinal forces of the vehicle (Fig. 3) include traction force F_{xf}, F_{xr} and rolling resistance F_{rf}, F_{rr} at the front/rear wheels respectively, aerodynamic resistance F_{r_air}, slope resistance F_{hc} with slope angle α, EV's inertia and are described in detail in the literature [18].

According to Fig. 3, the longitudinal dynamic of the vehicle is expressed:

$$(m+m_e)\dot{V}=(F_{xf}+F_{xr})-(F_{rf}+F_{rr}+F_{r\_\mathrm{air}}+F_{hc}), \quad (1)$$

where m and m_e are respectively the EV's mass and the equivalent mass of the electric drive rotating parts, kg; $\dot{V}$ is the vehicle acceleration, m/s^2.

$$m_e=\frac{1}{r_{wh}^2}\left\{J_{fwh}+J_{fd}+J_{gb}i_{fd}^2+J_m u_{gb}^2 i_{fd}^2\right\}, \quad (2)$$

where J_{fwh}, J_{fd}, J_{gb}, J_m are the inertia moment respectively of the front wheel assembly, final drive, transmission system, and electric motor, kg·m^2; i_{fd} is the final drive's transmission ratio, u_{gb} is the gearbox ratio.

Front and rear wheel dynamic submodels as well as the forces acting on them are shown in Fig. 4–7. The dynamic model of the active front wheel can be calculated by the following equation [18]:

$$J_{fwh}\dot{\omega}_{fwh}=T_{fdin}-F_{xf}r_{wh}-F_{zf}e_f-T_{bf}, \quad (3)$$

where ω_{fwh} is the front wheel's angular velocity, rad/s; T_{fdin}, T_{bf} are respectively the wheel active torque and the front wheel brake torque, N·m; $e_f = f_{rf}r_{wh}$ is the eccentricity of normal force F_{zf} (Fig. 2) at the vehicle front wheels, m; f_{rf} is rolling coefficient of front wheel, r_{wh} is dynamic wheel radius, m.

The formula for calculating the torque from the electric motor to the active wheel is built as follows:

$$T_{fdin}=T_{motor}u_{gb}\eta_{gb}i_{fd}\eta_{fd}, \quad (4)$$

where T_{motor} is the motor torque, N·m; η_{gb} is the gearbox efficiency; η_{fd} is the final drive's transmission efficiency.

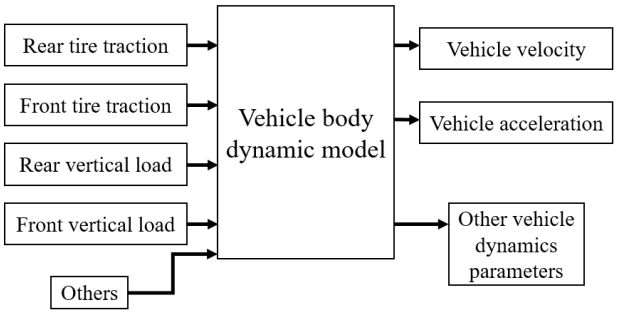

Fig. 2. Body vehicle dynamic model

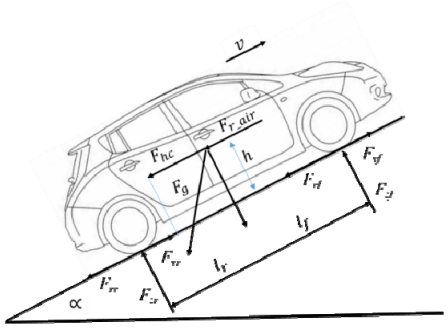

Fig. 3. The forces acting on the vehicle

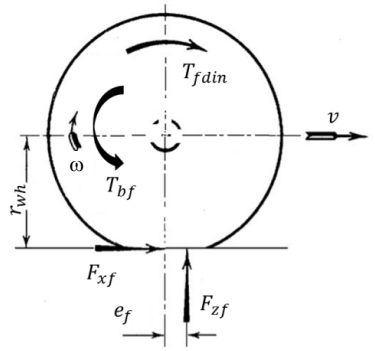

Fig. 4. The forces acting on the front wheel

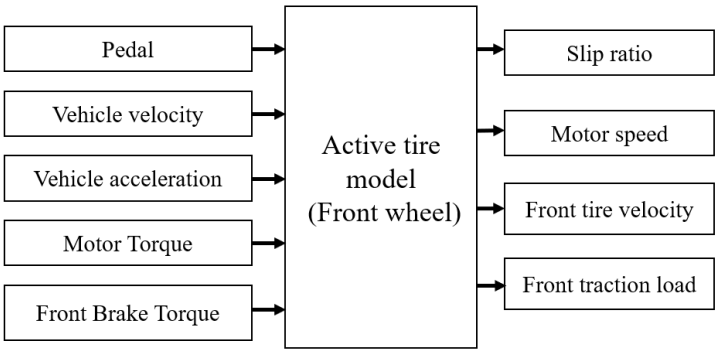

Fig. 5. Front wheel model

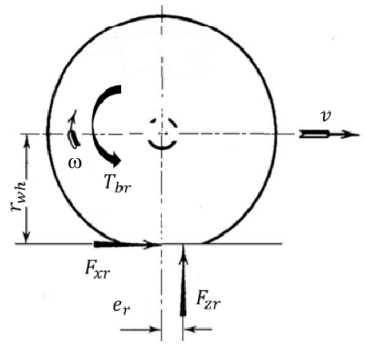

Fig. 6. The forces acting on the rear wheel

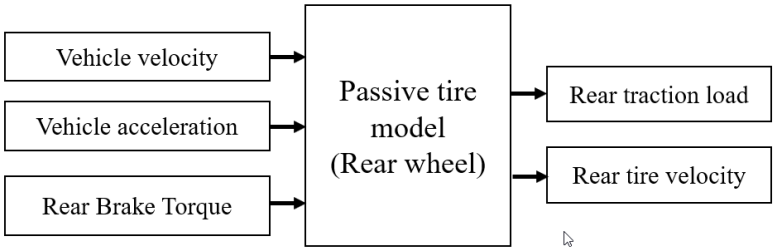

Fig. 7. Rear wheel model

The total moment of inertia relative to the front wheel is calculated as follows:

$$J_{fwh} = J_{whf} + J_{fd} + J_{gb} i_{gb}^2 + J_m i_{fd}^2 u_{gb}^2. \quad (5)$$

The rear wheel is the driven wheel, hence the forces acting on it are shown in Fig. 6.
The dynamic model of the passive rear wheel can be illustrated by the following equation [18]:

$$J_{rwh} \dot{\omega}_{rwh} = F_{xr} r_{wh} - T_{br} + F_{zr} e_r, \quad (6)$$

where J_{rwh} is the total moment of inertia relative to the rear wheel, kg·m^2, ω_{rwh} is the rear wheel's angular velocity, rad/s; $e_r = f_{rr} r_{wh}$ is the eccentricity of normal force F_{zr} (Fig. 2) at the vehicle rear wheels, m; f_{rr} is rolling coefficient of the rear wheel.

Tire submodel. According to the automotive theory [18], the maximum traction at the wheel is equal to the tire adhesive force. When the traction force provided by the electric motor acting on the wheel is higher than the adhesive force, a part of the traction force which is equal to the tire adhesive force propels the vehicle forward, while the rest is lost due to the tire slipping.

The equations for the calculation of the wheel slip ratio during the acceleration or braking process as well as the equations for determination of the corresponding traction forces F_{xf} and F_{xr} are well-known from the literary resource [18] and fully described in [7].

The reference slip ratio varies for the different tire characteristics and road adhesion conditions; therefore, to enhance the simulation accuracy a real-time reference slip ratio curve must be proposed. The relationship between the traction coefficient and tire slip ratio (Fig. 8) is determined empirically [7].

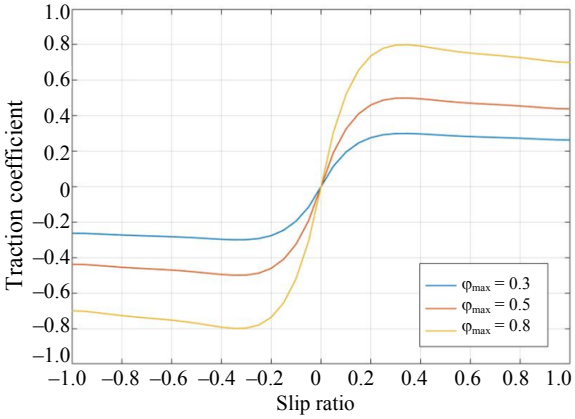

Fig. 8. The relationship between traction coefficient and tire slip ratio

Electric motor submodel based on the rotating permanent magnet electric motor (PMSM) with code number VFAAGB. The main PMSM's parameters and technical characteristics [19] and also the coefficients of piecewise function [17] for determining the efficiency in motor/generator mode are shown in Tab. 1 and 2.

Most electric motors are designed to run at 50 to 100 % of the rated load. Maximum efficiency is usually near 75 % of the rated load [20]. The efficiency of an electrical motor varies between 88 to 92 % for induction machines and from 93 to 95 % for synchronous motors [21].

The load and motor/generator efficiency relationship [17] are approximated by the piecewise function:

$$\begin{aligned} &\text{efficiency}(x) = \frac{c_1.x + c_2}{x + c_3} \left(0 \le x < 0.25\right); \\ &\text{efficiency}(x) = d_1.x + d_2 \left(0.25 \le x < 7.25\right); \\ &\text{efficiency}(x) = e_1.x + e_2 \left(x \ge 0.75\right), \end{aligned} \quad (7)$$

where $x = \frac{P_{motor}}{P_{rated}}$ denotes the ratio of the motor's mechanical power (P_{motor}) to the rated power (P_{rated}).

Table 1

Electric motor's parameters

Parameters, dimensionality	Value
Mass, *kg*	90,6
Rated torque, *N·m*	160
Time to reach the peak motor power, *s*	3
Rated efficiency, %	97
Rated power, kW	75

Table 2

Piecewise function coefficient

Coefficient	Motor mode	Generator mode
c_1	0,942269	0,942545
c_2	0,000061	0,000067
c_3	0,006118	0,006732
d_1	0,060000	0,057945
d_2	0,905000	0,904254
e_1	0,076000	0,066751
e_2	1,007000	1,002698

Obtained by equation (7) the load-efficiency curves in motor and generator modes are shown in Fig. 9.

The electric motor's maximum torque ($T_{\max}$) is presented as a function of the angular velocity. In most cases, when the motor's angular velocity is small, the torque is at the maximum and constant value. When the electric motor reaches the angular velocity limit (ω_c), the torque starts decreasing. In a PMSM, the torque decreases linearly with the increase of the angular velocity. The motor's torque is reduced while the motor's power remains unchanged [22, 23].

When the electric motor's angular velocity is lower than the limit ($\omega \le \omega_c$), the motor torque reaches the maximum value $T_c = T_{\max}$. When the electric motor's angular velocity is higher than the limit ($\omega > \omega_c$), the motor torque is inversely proportional to the motor speed $T_c = \dfrac{T_{\max}\omega_c}{\omega}$.

The electric motor drive characteristics and also its angular speed determination diagram are shown in the Fig. 10, 11.

The motor torque varies non-linearly according to each driving mode (Eco, Comfort, Sport) and depends on the accelerator pedal position (P_{in}). Assuming the relationship between P_{in} and $T_{\max}$ is a quadratic function:

$$T_{motor} = \left(aP_{in}^2 + bP_{in} + c\right)T_{\max}. \qquad (8)$$

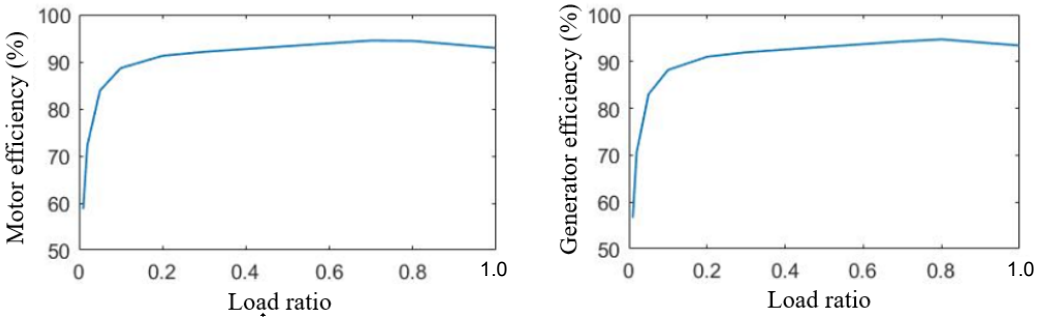

Fig. 9. The electric motor load-efficiency curve

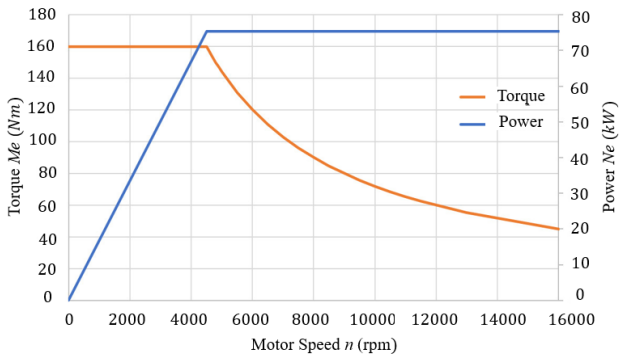

Fig. 10. The PMSM drive characteristics

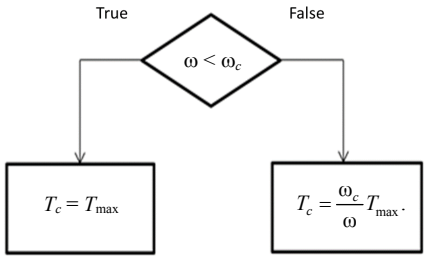

Fig. 11. The PMSM angular speed determination diagram

Assuming: $\frac{T_{motor}}{T_{\max}} = \%T_{\max}$.

Therefore: $\%T_{\max} = a\left(P_{in}\right)^2 + bP_{in} + c.$ (9)

In order to obtain the coefficients a, b, and c in different power unit driving modes, the real experiments on the dynamometer were conducted, the results of which are shown in this paper below.

Regenerative braking and battery submodels. During regenerative braking, the electric motor performs as a generator, converting the vehicle's kinetic energy into electrical energy, which is recharged in the EV battery. The regenerative brake model (Fig. 12) is built based on [7].

The traction accumulator battery model is built based on the documents [7, 17]. The battery equivalent circuit (Fig. 13) does not directly model the chemical characteristics inside the battery system, but it simulates the overall battery operation to calculate approximately the battery output parameters.

The driving cycle submodel provides the pedal signal by PID controller (Fig. 14). The driving cycle data are the standard driving cycles according to European standards with the following information: speed versus time, acceleration, and distance. These driving cycles are used to evaluate the EV's operating efficiency through energy consumption.

The input signal of this submodel (the variation between the desired and actual vehicle's speed) is processed in PID regulator to produce an output signal for simulating the driver's accelerator position with a value ranging from –1 to 1 corresponding to the combination of the actual acceleration signal (from 0 to 1) and the actual braking signal (from –1 to 0).

Dynamometer test results and mathematical model verification. Real experiments with VinFast Vf e34 passenger electric vehicle on a dynamometer test bench were carried out to determine the EV model input parameters and verify the mathematical model accuracy. Main vehicle technical specifications [19] are presented in Tab. 3, where the EV's mass center position was determined in the Automotive Dynamics Laboratory of the Hanoi University of Science and Technology (Vietnam).

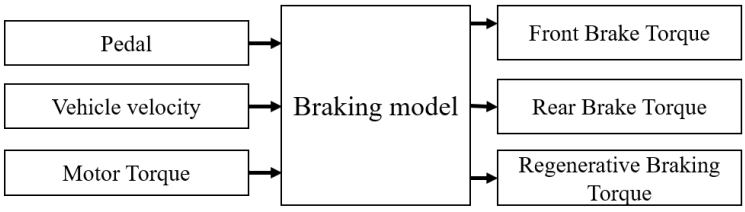

Fig. 12. Braking model

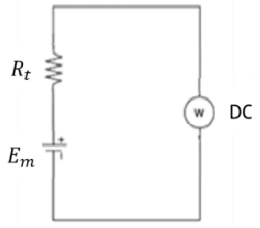

Fig. 13. Battery equivalent circuit:
R_t – internal resistance; E_m – open circuit voltage,
DC – battery direct current

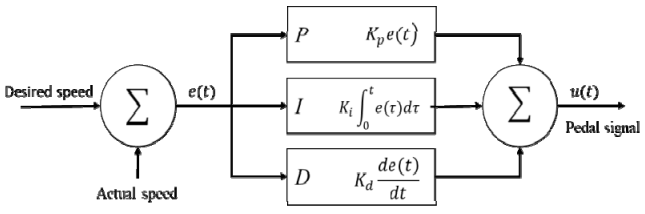

Fig. 14. Driving cycle submodel

Table 3

Technical specifications of VFe34-2020

Parameters	Value
Curb weight, kg	1490
Wheelbase, mm	2610.8
Overall dimension (L×W×H), mm	4300×1768×1613
Tire code	215/45R18
Gearbox transmission ratio	10.42
Motor rated power, kW	75
Motor rated torque, N·m	160
Battery type	Li-on
Battery capacity, kW·h	41.58
Battery nominal voltage, V	400
Battery amperage, A·h	103.38
Gravity center/front axle distance, m	1.118
Gravity center/rear axle distance, m	1.493
Height of gravity center, m	0.649

The EV motor characteristics in different operating modes (Eco, Comfort, Sport) are determined on the AHS MULTIFLEX EASY dynamometer [24]. This stand allows the operator to adjust the wheel's drag power and to measure the drive wheel's velocity and tractive force (F_x) according to different accelerator pedal positions:

$$T_{motor} = \frac{F_x r_{wh}}{i\eta}, \qquad (10)$$

where F_x is the traction force at the wheel, N; i, η are the gear ratio and the efficiency of the transmission system; r_{wh} is the wheel radius, m.

Such experiments were conducted in different operating modes (Eco, Comfort, Sport) with two pedal positions of 50 and 100 %. The results of experiments (Tab. 4) were used for determination with the help of equations (8)–(9) of the relationship between the accelerator pedal position and motor torque in different driving modes (Fig. 15).

Table 4

Torque parameters of the electric motor

Eco			Comfort			Sport		
P_{in}	T_{motor}, $N{\cdot}m$	$\%T_{\max}$	P_{in}	T_{motor}, $N{\cdot}m$	$\%T_{\max}$	P_{in}	T_{motor}, $N{\cdot}m$	$\%T_{\max}$
0.5	34	0.213	0.5	52	0.325	0.5	139	0.869
1	160	1	1	160	1	1	160	1

In order to verify the above-mentioned model's accuracy, some experiments were carried out to measure the power and longitudinal force on the vehicle's drive wheels at different driving speeds [24]. Then, these measurement results are compared with the simulation results to evaluate the model's accuracy.

Since the experimental devices cannot simulate the inertial force acting on the vehicle, the experiments are performed in the zero inertial resistance condition or, in other words, at the constant velocity. The air and rolling resistance are constant and the slope resistance varies, but the total drag force at the constant speed in both simulation and experiment must be equal.

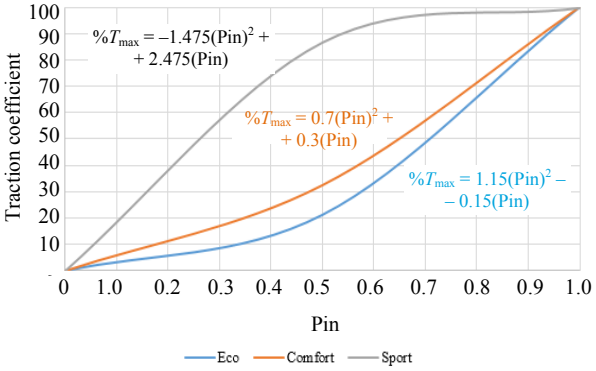

Fig. 15. The electric motor characteristics in several driving modes

During the different operating modes (Eco, Comfort, Sport) the accelerator pedal is held at 50 %, according to the data obtained from the OBD-II communication port, and the wheel load varies to achieve the desired speed. The simulation and experimental results are shown in Tab. 5.

The experimental and simulated results show a large deviation (letter than 10 %) when the vehicle is running in the SPORT mode, and this deviation increases as the vehicle velocity gets higher. This is due to the slip on the dynamometer's rollers when the motor generates high torque and power. In the other driving modes, the deviation between the simulation and the experiment's results is low and does not exceed 4 % thus ensuring the accuracy of the EV model and its reliability for future research.

Table 5

Simulation and experimental results

Operating modes	V, km/h			F_x, N			P, kW		
	Simulation	Experiment	Error (%)	Simulation	Experiment	Error (%)	Simulation	Experiment	Error (%)
Eco	75.94	76	**0.08**	640.2	640	**0.03**	13.50	14	**3.54**
	62.20	62	**0.32**	779.1	800	**2.61**	13.46	13.8	**2.46**
	53.80	54	**0.37**	897.9	900	**0.23**	13.42	13.8	**2.76**
Comfort	77.90	78	**0.12**	1023	1000	**2.30**	22.14	22	**0.64**
	60.80	60	**0.45**	1302	1300	**0.15**	21.99	22	**0.05**
	51.24	51	**0.47**	1448	1400	**3.43**	20.60	20	**3.05**
Sport	81.66	82	**0.41**	2254	2460	**8.37**	51.10	56.0	**8.75**
	66.80	67	**0.30**	2760	2950	**6.44**	51.20	54.9	**6.72**
	46.70	47	**0.64**	3780	4050	**6.67**	49.00	52.9	**7.26**

Besides, the EV model's accuracy was evaluated by comparison in terms of the NEDC vehicle driving distance at a full battery charge in simulation mode and real experiments. According to VinFast technical information [25] passenger electric vehicle VF e34 can travel in the NEDC a distance of 285 km on a full battery state of charge (100 % SOC). In order to measure the maximum VF e34 driving NEDC distance the simulation was repeated many times until the battery's SOC dropped up to 0 %. The results of such an experiment show a small deviation of less than 5 % between the NEDC driving distance of 272,14 km in simulation mode and VinFast manufacturer's claim of 285 km, which confirms the high accuracy of the EV model. Hence, this model is reliable for performing further vehicle evaluation.

Simulation results

The proposed EV model is used to analyze the influence of the adhesion coefficient on the EV's energy consumption and driving dynamics in the following cases: acceleration based on RAMP-pattern [26] or operation in standard driving cycles.

Acceleration based on RAMP-pattern. The EV's acceleration from 0 to 100 km/h with different RAMP levels (t_{ramp}) in Comfort driving mode with different road adhesion coefficients of 0.3, 0.5, and 0.8 were investigated. In this case, the time t_{ramp} required to increase the accelerator level from 0 to 1 was varied in the range from 2 to 16 seconds with 2-second intervals. The adhesion coefficient's influence on vehicle dynamics is analyzed based on 2 criteria: acceleration time and energy consumption. The simulation results of the acceleration tests with different adhesion coefficients are shown in Fig. 16, 17.

As can be seen from the research results the acceleration time required for the vehicle to reach 100 km/h increases with the rise of the RAMP step (t_{ramp}). However, the vehicle consumes less energy as the RAMP step increases. On the roads with a high adhesion coefficient of 0.8 the acceleration time difference between extreme RAMP values is approximately 10 *s*, which is 56.4 % (the acceleration time is 16.2 *s* with 2 *s*-RAMP step and 25.34 *s* with 16 *s*-RAMP step). In this case, from the point of energy consumption view, there is no significant difference in terms, only 0.07 km/(kW·h), which is 8.0 %. This shows that under conditions with a high adhesion coefficient, the RAMP step shows less impact on the EV's energy consumption.

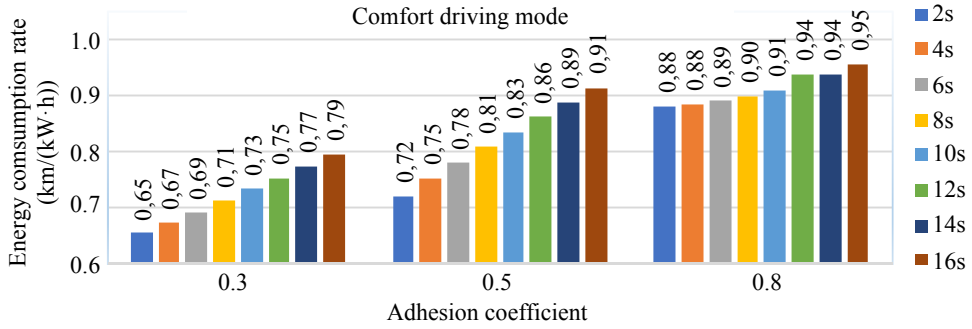

Fig. 16. Energy consumption comparison chart at RAMP-pattern EV acceleration

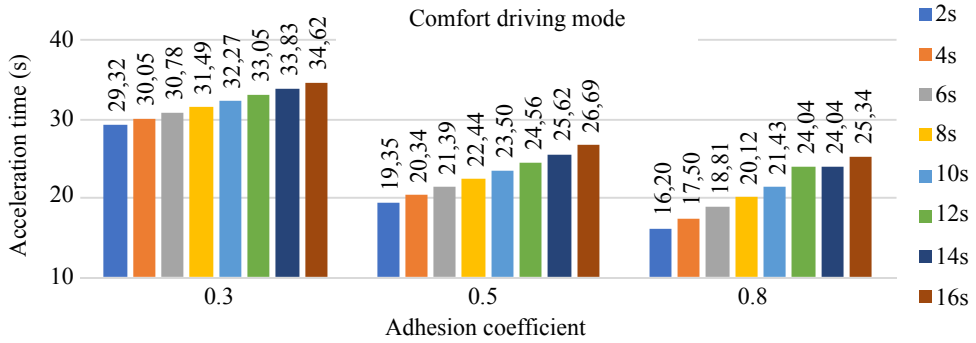

Fig. 17. Acceleration time comparison chart at RAMP-pattern EV acceleration

On roads with a low adhesion coefficient of 0.3, in which the wheels are prone to slipping, the variation of acceleration times between the lowest and highest RAMP steps are almost halved of those in a high adhesion coefficient condition (acceleration time in 2 *s*-RAMP step is only about 5.3 *s* longer than 16 *s*-RAMP step, corresponding to 18.1 %), but the energy consumption is twice as high as that in the high adhesion coefficient condition, at 0.14 km/(kW·h) (corresponding to 21,5 %). This shows that under the low adhesion coefficient condition, the accele-ration method does not have much influence on the acceleration time.

The above test results are fully compatible with the laws of physics when vehicles run on roads with different adhesion coefficients.

Road adhesion coefficient impact on EV's energy consumption in different driving cycles. The time-speed graph of the standard driving cycles [27, 28], such as HWFET, ArtURBAN, NEDC and NYCC, are presented in Fig. 18. The characteristic parameters [29] of the above driving cycles are shown in Tab. 6.

Based on the above presented information the EV's energy consumption in different standard driving cycles was investigated in order to evaluate the EV's energy saving capability in Comfort driving mode with different adhesion coefficients. The simulation results of the energy consumption rate are shown in Fig. 19.

The research results shows that on the road with a high adhesion coefficient of 0.8 the low tire slipping ratio occurs. Hence, the energy consumption slightly changed under different driving cycles, ranging from 6.06 to 6.53 km/(kW·h). Thus, the EV's energy economy is stable under different operating conditions.

On roads with low adhesion coefficients of 0.5 and 0.3, the energy consumption rate dropped significantly in the inner-city driving cycles (NYCC and ArtUrban). On the road with an adhesion coefficient of 0.5 the energy consumption is half of that in the high adhesion coefficient. On the road with an adhesion coefficient of 0.3 the energy consumption is even lower, about one-fifth of that in the high adhesion coefficient. In contrast, in the high-speed driving cycles (HWFET and NEDC), the energy consumption is similar to those in the high adhesion coefficient condition.

The variation in the energy consumption in the NYCC and ArtUrban when varying the adhesion coefficient can be explained as follows: Those urban driving cycles have low average speed, velocity ratio and high acceleration characteristics (Tab. 6), so the RAMP steps are small at each acceleration and braking, which means that the vehicle operates under continuous acceleration and braking conditions. At this time energy is consumed due to the tire slipping when the road's adhesion coefficient is low.

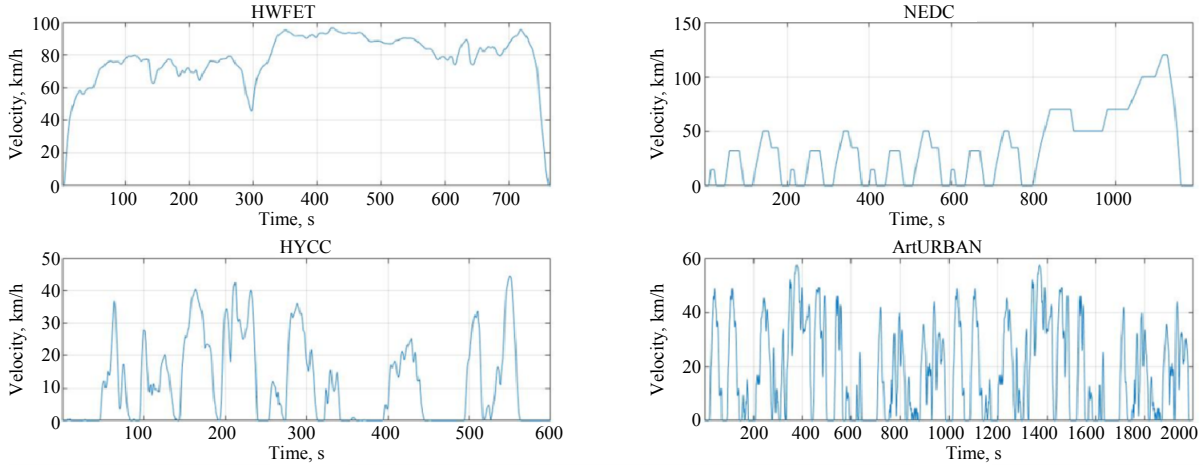

Fig. 18. Survey driving cycles

Table 6

Characteristic parameters of the standard driving cycles

Driving Cycle	Average velocity V_{avg}, m/s	Root-mean-cube velocity V_{rmc}, m/s	Velocity ratio Λ	Characteristic acceleration ã, m/s^2
NYCC	3.16	5.73	1.81	0.293
HWFET	21.45	22.22	1.04	0.069
NEDC	9.18	14.89	1.62	0.112
ArtURBAN	4.90	7.93	1.62	0.313

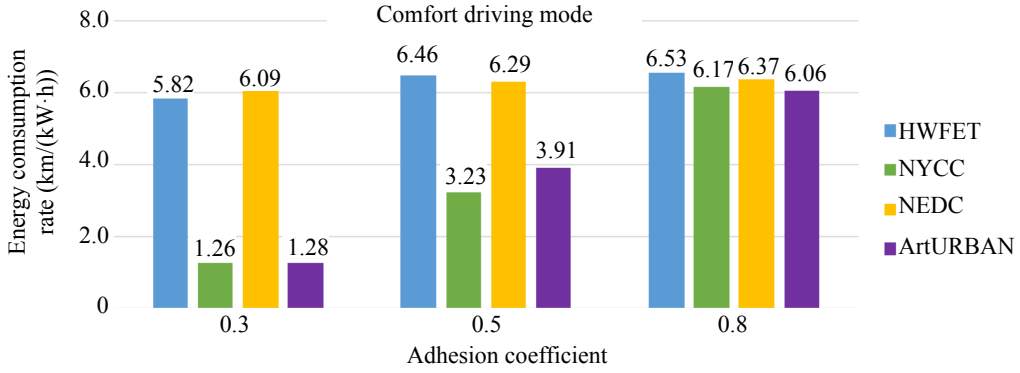

Fig. 19. Energy consumption rate at different driving cycles

In the high-speed driving cycle (HWFET) the first acceleration phase is a small RAMP step, while the rest of the driving cycle shows stable acceleration and speed, hence the energy consumption is independent of the road adhesion coefficient. In the NEDC cycle, although acceleration and braking are frequent, the tire slipping occurs less frequently, even in the low adhesion coefficient due to high RAMP steps. Therefore, high energy consumption is achieved even in low adhesion coefficient roads.

CONCLUSIONS

1. The EV model with different driving modes was built and its results were compared with the empirical data for the model's verification. The error between the simulation and experiment in terms of the driving distance in NEDC is less than 10 %, and those errors in terms of tire dynamics are less than 4% with ECO driving mode and less than 9 % with SPORT driving mode. These aforementioned number ensures the model's accuracy and its possibility for further research about the vehicle dynamics and energy efficiency comparison with different tire adhesion coefficients without conducting complex experiments.

2. Simulation results show that on a road with a high adhesion coefficient of 0.8 the acceleration time from 0 to 100 km/h depends heavily on the driver's depression intensity on the accelerator pedal, with a maximum variation of up to 56.4 %; however, the energy consumption is less dependent on the acceleration time, with the maximum variation of 8.0 %. In contrast, on a road with a low adhesion coefficient, the acceleration time is less dependent on the driver's depression intensity on the accelerator pedal, with a maximum variation of up to 18.1 %; however, the energy consumption is more dependent on the acceleration time, with the maximum variation of 21.5%, which is twice more than that on high adhesion coefficient road.

3. On standard driving cycles with high traction coefficients, there is not much difference in energy consumption, which shows the stable operation of EVs in different traffic conditions. On driving cycles with high braking frequency and acceleration, such as NYCC and ArtURBAN, the energy consumption fluctuates considerably to the decrease of the adhesion coefficient, with a maximum variation of five times; however, on the driving cycles with low braking frequency and acceleration, such as HWFET and NEDC, there are no significant changes in the energy consumption.

Funding: This research was funded by the Hanoi University of Science and Technology, grant number T2023-PC-023.

REFERENCES

1. Bloomberg New Energy Finance. *Electric Vehicle Outlook 2021 Executive Summary* Available at: https://bnef.turtl.co/story/evo-2021/page/1?teaser=yes (accessed 05 December 2023).
2. Le V. N., Dam H. P., Duong N. K., Hoang M. H. (2022) An Average Method for Calculating the Vehicle Energy Consumption on Driving Cycles. *International Review of Mechanical Engineering (IREME),* 16, 610–619. https://doi.org/10.15866/ireme.v16i12.22954.
3. Adrian F., Antoneta I. B., Iulian M., Seddik B. (2012) Energy Management System within Electric Vehicles Using Ultracapacitors: An LQG-Optimal-Control-Based Solution. *IFAC Proceedings Volumes*, 45 (25), 229–234. https://doi.org/10.3182/20120913-4-IT-4027.00033.
4. Liu K., Wang J., Yamamoto T., Morikawa T. (2018) Exploring the Interactive Effects of Ambient Temperature and Vehicle Auxiliary Loads on Electric Vehicle Energy Consumption. Applied Energy, 227, 324–331. https://doi.org/ 10.1016/j.apenergy.2017.08.074.
5. Viswanathan V., Palaniswamy L. N., Leelavinodhan P. B. (2019) Optimization Techniques of Battery Packs Using

Re-Configurability: A Review. *Journal of Energy Storage*, 23, 404–415. https://doi.org/10.1016/j.est.2019.03.002.
6. Zhu W. (2022) Optimization Strategies for Real-Time Energy Management of Electric Vehicles Based on LSTM Network Learning. *Energy Reports*, 8 (8), 1009–1019. https://doi.org/10.1016/j.egyr.2022.10.349.
7. Le V. N., Dam H. P., Nguyen T. H., Kharitonchik S. V., Kusyak V. A. (2023) Research of Regenerative Braking Strategy for Electric Vehicles. *Energetika. Izvestiya Vysshikh Uchebnykh Zavedenii i Energeticheskikh Ob'edinenii SNG = Energetika. Proceedings of CIS Higher Education Institutions and Power Engineering Associations*, 66 (2), 105–123. https://doi.org/10.21122/1029-7448-2023-66-2-105-123.
8. Andreas B., Wolfgang R. (2017) The influence of Driving Patterns on Energy Consumption in Electric Car Driving and the Role of Regenerative Braking. *Transportation Research Procedia*, 22, 174–182. https://doi.org/10.1016/j.trpro.2017.03.024.
9. Revathy R., Balaji B., Mohasin A. K. A., Gobinath A. (2023) Supercapacitor and BLDC Motor-Based Regenerative Braking for an Electric Vehicles. *2nd International Conference on Smart Technologies and Systems for Next Generation Computing (ICSTSN)*. Villupuram, India, 1–5. https://doi.org/10.1109/ICSTSN57873.2023.10151546.
10. Kubaisi R., Gauterin F., Giessler M. (2014) A Method to Analyze Driver Influence on the Energy Consumption and Power Needs of Electric Vehicles. *IEEE International Electric Vehicle Conference (IEVC)*. Florence, Italy, 1–4. https://doi.org/10.1109/IEVC.2014.7056215.
11. Carreón-Sierra S., Salcido A. (2022) Effects of Driving Style on Energy Consumption and CO_2 Emissions. Collective Dynamics, 7, 1–34. https://doi.org/10.17815/CD.2022.137.
12. Rodolfo R. (2020) A Study on the Impact of Driver Behavior on the Energy Consumption of Electric Vehicles in a Virtual Traffic Environment: Master's Thesis in the University of Michigan. Dearborn, USA. 84.
13. Leontiev D. N., Bogomolov V. A., Klymenko V. I., Ryzhyh L. A., Lomaka S. I., Suhomlin A. V., Kuripka A. V., Frolov A. A. (2022) About Braking of Wheeled Vehicle Equipped with Automated Brake Control System. *Nauka i Tehnika = Science & Technique,* 21 (1), 63–72. https://doi.org/10.21122/2227-1031-2022-21-1-63-72 (in Russian).
14. Leontiev D. N., Nikitchenko I. N., Ryzhyh L. A., Lomaka S. I., Voronkov O. I., Hritsuk I. V., Pylshchyk S. V., Kuripka O. V. (2019) About Application the Tyre-Road Adhesion Determination of a Vehicle Equipped with an Automated System of Brake Proportioning. *Nauka i Tehnika = Science & Technique,* 18 (5), 401–408. https://doi.org/10.21122/2227-1031-2019-18-5-401-408 (in Russian).
15. Li L., Song J., Li H. Z., Shan D. S., Kong L., Yang C. C. (2009) Comprehensive Prediction Method of Road Friction for Vehicle Dynamics Control. *Proceedings of the Institution of Mechanical Engineers, Part D: Journal of Automobile Engineering*, 223 (8), 987–1002. https://doi.org/10.1243/09544070JAUTO1168.
16. Konstantinos, N. G., Mitrentsis G. (2017) A Computationally Efficient Simulation Model for Estimating Energy Consumption of Electric Vehicles in the Context of Route Planning Applications. *Transportation Research Part D: Transport and Environment*, 50, 98–118. https://doi.org/10.1016/j.trd.2016.10.014.
17. Le T. N., Dinh B. T., Pham V. S., Le V. T., Nguyen T. D., Nguyen T. L., Nguyen T. D. (2021) Research on Building an Electric Car Model. *Sustainable Energy. Student Forum*. Hanoi, Viet Nam, 514–520.
18. Vo V. H., Nguyen T. D., Ta T. H. (2021) *Modern Automotive Theory*. Hanoi, Vietnam Education Publishing House Limited Company. 210.
19. VF e34. *Vinfast*. Available at: https://shop.vinfastauto.com/vn_en/dat-coc-xe-dien-vfe34.html (accessed 25 August 2023).
20. Department of Energy USA (1997) *Determining Electric Motor Load and Efficiency*. Available at: https://energy.gov/eere/amo/downloads/determining-electric-motor-load-and-efficiency#:~:text=Most%20electric%20motors%20are%20designed,dramatically%20below%20about%2050%25%20load (accessed 23 August 2023).
21. Vodovozov V., Raud Z., Lehtla T., Rassolkin A., Lillo N. (2014) Comparative Analysis of Electric Drives Met for Vehicle Propulsion. *Ninth International Conference on Ecological Vehicles and Renewable Energies (EVER).* Monte-Carlo, Monaco, 1–8. https://doi.org/10.1109/EVER.2014. 6844125.
22. Ngo P., Gulkov G. I. (2017) Calculation of a Mechanical Characteristic of Electric Traction Motor of Electric Vehicle. *Energetika. Izvestiya Vysshikh Uchebnykh Zavedenii i Energeticheskikh Ob'edinenii SNG = Energetika. Proceedings of CIS Higher Education Institutions and Power Engineering Associations,* 60 (1), 41–53. https://doi.org/10. 21122/ 1029-7448-2017-60-1-41-53 (in Russian).
23. Ngo P. (2017) Calculation of Inductance of the Interior Permanent Magnet Synchronous Motor. *Energetika. Izvestiya Vysshikh Uchebnykh Zavedenii i Energeticheskikh Ob'edinenii SNG = Energetika. Proceedings of CIS Higher Education Institutions and Power Engineering Associations,* 60 (2), 133–146. https://doi.org/10.21122/1029-7448-2017-60-2-133-146 (in Russian).
24. AHS MULTIFLEX EASY. *AHS Prüftechnik*. Available at: https://www.xn--ahs-prftechnik-lsb.de/produkte/rollen brems pruefstaende-pkw/ahs-multiflex-easy/ (accessed 25 August 2023).
25. How Many Kilometers Can the VinFast VF e34 Electric Car Travel on a Full Charge? *Vinfast*. Available at: https://vinfastauto.com/vn_vi/vf-e34-di-duoc-bao-nhieu-km (accessed 25 August 2023).
26. Ferrarin M., Pedotti A. (2000) The Relationship Between Electrical Stimulus and Joint Torque: a Dynamic Model. *IEEE Transactions on Rehabilitation Engineering,* 8 (3), 342–352. https://doi.org/10.1109/86.867876.
27. Zhang B., Yang F., Teng L., Ouyang M., Guo K., Li W. (2019) Comparative Analysis of Technical Route and Market Development for Light-Duty PHEV in China and the US. *Energies*, 12, 3753. https://doi.org/10.3390/en12193753 9-2019.
28. Mallouh M., Surgenor B. W., Mohammad S., Abdelhafez E., Hamdan A., Mohammad A. H. (2014) Performance Comparison of Different Power Management Control Strategies for a Hybrid Fuel Cell/Battery Vehicle. *ASME 2014 12th Biennial Conference on Engineering Systems Design and Analysis, July 25–27, 2014*, *Vol. 1.* 5 p. https://doi. org/10.1115/ESDA2014-20599.
29. IMEE (2019) *Standardized Drive Cycles*. Available at: https://imee.pl/pub/drive-cycles (accessed 25 August 2023).

Received: 21.11.2023
Accepted: 23.01.2024
Published online: 29.03.2024